The Astrophysical Journal, 592:L67–L70, 2003 August 1

EUROPIUM ISOTOPE RATIOS IN *s*-PROCESS ELEMENT–ENHANCED METAL-POOR STARS: A NEW PROBE OF THE ^{151}Sm BRANCHING[1]

Wako Aoki,[2] Sean G. Ryan,[3] Nobuyuki Iwamoto,[2,4] Timothy C. Beers,[5] John E. Norris,[6] Hiroyasu Ando,[2] Toshitaka Kajino,[2] Grant J. Mathews,[7] and Masayuki Y. Fujimoto[8]

Received 2003 May 22; accepted 2003 June 23; published 2003 July 7

ABSTRACT

We report on the first measurement of the Eu isotope fractions (^{151}Eu and ^{153}Eu) in *s*-process element–enhanced metal-poor stars. We use these ratios to investigate the ^{151}Sm branching of *s*-process nucleosynthesis. The measurement was made by detailed study of Eu II lines that are significantly affected by hyperfine splitting and isotope shifts in spectra of the carbon-rich very metal poor stars LP 625−44 and CS 31062−050, observed with the Subaru Telescope High Dispersion Spectrograph. The ^{151}Eu fractions [fr(^{151}Eu) = ^{151}Eu/(^{151}Eu + ^{153}Eu)] derived for LP 625−44 and CS 31062−050 are 0.60 and 0.55, respectively, with uncertainties of about ±0.05. These values are higher than found in solar system material but agree well with the predictions of recent *s*-process models. We derive new constraints on the temperature and neutron density during the *s*-process based on calculations of pulsed *s*-process models for the ^{151}Eu fraction.

Subject headings: nuclear reactions, nucleosynthesis, abundances — stars: abundances — stars: AGB and post-AGB — stars: Population II

1. INTRODUCTION

The slow neutron capture process (*s*-process) is responsible for about half of the abundances of elements heavier than the iron peak in solar system material. The *s*-process traditionally has been described by two approaches: the schematic classical approach (e.g., Käppeler, Beer, & Wisshak 1989) and modeling of the *s*-process in thermally pulsing asymptotic giant branch (AGB) stars (e.g., Straniero et al. 1995). In the classical approach, the neutron exposure is estimated from the abundance patterns of pure *s*-process isotopes in solar system material or the elemental abundance patterns in stars enriched in *s*-process elements, while the temperature and neutron density during the *s*-process can be estimated by an analysis of the branchings of the neutron capture chains where the rates for beta decay and neutron capture are comparable.

For ^{151}Sm, whose half-life is about 90 yr, the β-decay rate is strongly dependent on temperature, while the neutron capture rate is not. This makes the ^{151}Sm branching an excellent thermometer (e.g., Wisshak et al. 1995). Previously, this branching has been analyzed using the ^{152}Gd and ^{154}Gd isotope ratios in solar system material, which are believed to be significantly affected by this branching (e.g., Beer & Macklin 1988; Wisshak et al. 1995). One difficulty in this approach is that these Gd isotopes are affected by a small amount of contamination from the *p*-process, although they are shielded from the *r*-process. Hence, an independent observational constraint on the branching is desired.

The Eu isotope ratio (^{151}Eu/^{153}Eu) is one possible constraint. More than 90% of Eu in the solar system is provided by *r*-process nucleosynthesis (e.g., Käppeler et al. 1989; Arlandini et al. 1999; Burris et al. 2000), which suggests that it is difficult to constrain the *s*-process from measurement of the Eu isotopes in *solar system material*. However, the Eu isotope ratios can also be measured in individual stars, as high-resolution spectroscopy can partially resolve the expected hyperfine splitting and isotope shifts. Sneden et al. (2002) and Aoki et al. (2003) analyzed the Eu isotopes for *r*-process element–enhanced stars. They showed that the isotope ratios derived for a total of four of these objects agree well with that in solar system material. In this Letter, we apply this analysis to two *s*-process element–enhanced metal-poor stars and report the first results of our analysis of Eu isotopes to analyze the ^{151}Sm branching.

2. OBSERVATIONS

We selected two subgiants (LP 625−44 and CS 31062−050), which were found to be enriched in *s*-process elements in our previous studies (Aoki et al. 2000, 2002a) as most suitable for this investigation. These stars are both very metal poor ([Fe/H] = −2.7 and −2.4, respectively[9]) and have quite similar atmospheric parameters, as shown in Table 1. The observed enhancement of *s*-process elements in these stars is believed to be due to nucleosynthesis in extinct AGB stars that transferred mass to the surviving luminous companions of the binary systems. The binarity of these stars is discussed below. The enhancement of the bulk of the *s*-process elements in these two stars is also similar (e.g., [Ba/Fe] ∼ +2.5). One important difference between these two objects is their Pb abundance: the Pb/Ba ratio in CS 31062−050 is 5 times higher than that in LP 625−44. For comparison purposes, we also selected a very metal deficient giant, HD 6268 ([Fe/H] = −2.5), which exhibits a moderate enhancement of *r*-process elements and has

[1] Based on data collected at the Subaru Telescope, which is operated by the National Astronomical Observatory of Japan.

[2] National Astronomical Observatory, 2-21-1, Osawa, Mitaka, Tokyo 181-8588, Japan; aoki.wako@nao.ac.jp, ando@optik.mtk.nao.ac.jp, kajino@nao.ac.jp.
[3] Department of Physics and Astronomy, Open University, Walton Hall, Milton Keynes MK7 6AA, UK; s.g.ryan@open.ac.uk.
[4] Current address: Department of Astronomy, School of Science, University of Tokyo, Hongo, Bunkyo-ku, Tokyo 133-0033, Japan; niwamoto@astron.s.u-tokyo.ac.jp.
[5] Department of Physics and Astronomy, Michigan State University, East Lansing, MI 48824-1116; beers@pa.msu.edu.
[6] Research School of Astronomy and Astrophysics, Australian National University, Mount Stromlo Observatory, Cotter Road, Weston ACT 2611, Australia; jen@mso.anu.edu.au.
[7] Department of Physics, Center for Astrophysics, University of Notre Dame, 225 Nieuwland Science Hall, Notre Dame, IN 46556; gmathews@nd.edu.
[8] Department of Physics, Hokkaido University, Sapporo, Hokkaido 060-0810, Japan; fujimoto@astro1.sci.hokudai.ac.jp.

[9] [A/B] ≡ log (N_A/N_B) − log (N_A/N_B)$_\odot$, and log ϵ_A ≡ log (N_A/N_H) + 12 for elements A and B.

TABLE 1
PROGRAM STARS AND OBSERVATIONS

Star	Exposure[a]	Signal-to-Noise Ratio[b]	Observation Date (JD)	Radial Velocity (km s^{-1})	$T_{\rm eff}$/ log g/[Fe/H]/$v_{\rm micro}$	$v_{\rm macro}$ (km s^{-1})
LP 625−44	270 (9)	137	2002 Aug 22 (2,452,509)	28.41 ± 0.19	5500/2.5/−2.7/1.2	6.69 ± 0.13
CS 31062−050	390 (13)	124	2002 Aug 23 (2,452,510)	11.51 ± 0.17	5600/3.0/−2.4/1.3	5.30 ± 0.40
HD 6268	100 (5)	304	2002 Aug 22 (2,452,509)	40.13 ± 0.15	4600/1.0/−2.5/2.1	7.27 ± 0.27

[a] Total exposure time (in minutes) and number of exposures.
[b] Signal-to-noise ratio per 0.012 Å pixel at 4000 Å.

strong Eu lines, comparable to those in the two *s*-process element–enhanced stars.

The [Ba/Eu] values of LP 625−44 and CS 31062−050 derived in our previous studies (Aoki et al. 2002a, 2002b) are 1.09 and 0.46, respectively. These are more than 1 dex higher than the value of the *r*-process component in solar system material (−0.69; Arlandini et al. 1999). While the [Ba/Eu] value of LP 625−44 is similar to that of the solar system *s*-process component (+1.15), the value of CS 31062−050 is significantly lower. However, low [Ba/Eu] values (∼0.4) are predicted by some AGB nucleosynthesis models (e.g., Goriely & Mowlavi 2000) for metal-deficient stars, for which high neutron exposure is expected because of the high ratios of neutrons per seed nuclei. Indeed, the value of [Ba/Eu] ∼ 0.4 is not unusual in carbon-rich metal-deficient stars such as CS 31062−050 (e.g., Aoki et al. 2002a; Johnson & Bolte 2002). To explain these [Ba/Eu] values by contamination from the *r*-process, we must assume a very large enhancement of *r*-process elements ([Eu/Fe] ∼ +1.5–1.8), similar to that in extremely *r*-process–enhanced stars, such as CS 31082−001 (Cayrel et al. 2001), which are known to be quite rare. For these reasons, we assume in the following discussion that the majority of the Eu in CS 31062−050, as well as in LP 625−44, originates from the *s*-process.

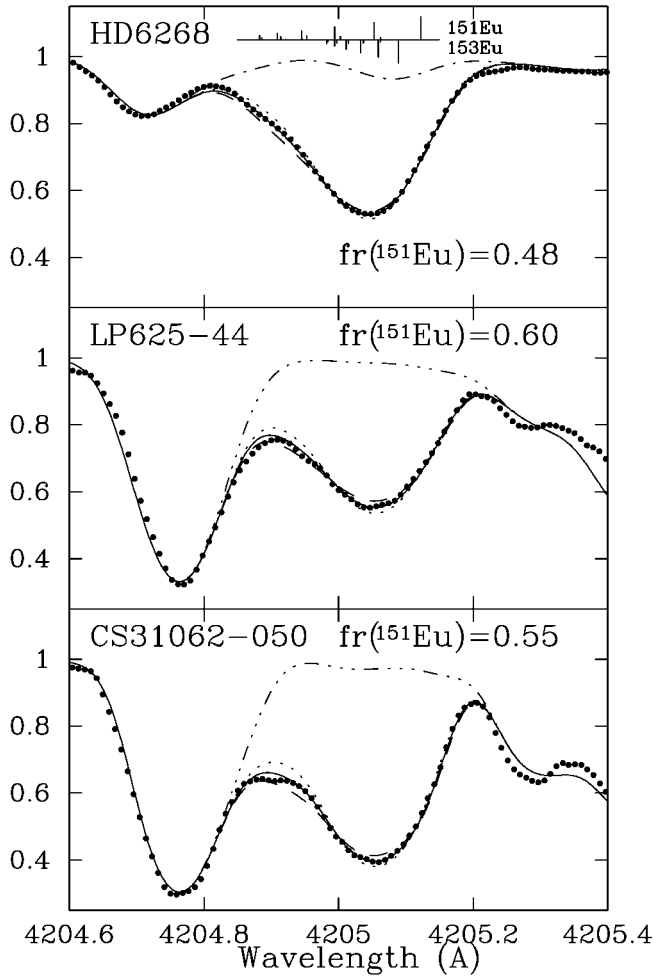

FIG. 1.—Comparison of the observed spectra (*filled circles*) and synthetic ones (*lines*) for the Eu II 4205 Å line. The name of the object and the adopted fr(^{151}Eu) value are presented in each panel. The solid line shows the synthetic spectra for the adopted fr(^{151}Eu); the dotted and dashed lines show those for ratios that are smaller and larger by 0.10 in fr(^{151}Eu), respectively. The dot-dashed lines show the synthetic spectra for no Eu. The weak blending at 4205.09 Å in the spectrum of HD 6268 (*top*) is due to V II, whose effect is negligible in the two subgiants. The wavelengths and relative strength of the hyperfine components for ^{151}Eu and ^{153}Eu are shown in the top panel.

The observations that we report here were made with the Subaru Telescope High Dispersion Spectrograph (HDS; Noguchi et al. 2002) in 2002 August. The wavelength range covered was 3100–4700 Å, with a resolving power $R = 90{,}000$. The total exposure times and signal-to-noise ratios obtained are listed in Table 1.

The heliocentric radial velocities measured for our spectra are given in Table 1. Aoki et al. (2000) already reported a variation of radial velocities for LP 625−44, which is confirmed by the present measurement. For CS 31062−050, a change of radial velocity from the previous measurement ($V_r = 7.75$ km s^{-1} by Aoki et al. 2002a) was also detected. These results suggest the binarity of these stars and strongly support the mass transfer scenario for the enrichment of *s*-process elements.

3. ANALYSIS AND RESULTS

We adopted the Eu line data, including the hyperfine splitting and isotope shifts, provided by Lawler et al. (2001). The isotope fractions of ^{151}Eu [fr(^{151}Eu) = ^{151}Eu/(^{151}Eu + ^{153}Eu)] were measured by fitting observed spectra with synthetic ones calculated for the Eu lines, using the model atmospheres of Kurucz (1993) and atmospheric parameters derived in the previous studies (Aoki et al. 2002a, 2002b). The macroturbulent velocity was estimated by fitting a Gaussian profile to clean Fe and Ti lines detected in the same spectrum for each object (see Table 1). Our careful investigation of the HDS instrumental profiles around the Eu lines used in the analysis showed that the profile is quite symmetric. Hence, a Gaussian profile approximation is sufficient for the analysis of stellar spectra that are further broadened by macroturbulence.

Figure 1 shows the spectra of the Eu II λ4205 line in our three program stars. In the calculation of synthetic spectra, blending by other species is included using the comprehensive line list of Kurucz & Bell (1995) and the CH and CN line lists produced in Aoki et al. (2002a). The dot-dashed lines show the synthetic spectra calculated without the Eu II contribution. The absorption around 4205 Å is dominated by Eu II. In the top panel, the line positions of both Eu isotopes are shown. Since the hyperfine

TABLE 2
RESULTS

	HD 6268		LP 625−44		CS 31062−050	
LINE	fr(^{151}Eu)	log ϵ(Eu)	fr(^{151}Eu)	log ϵ(Eu)	fr(^{151}Eu)	log ϵ(Eu)
λ3819	0.44 ± 0.11	−1.55	0.68 ± 0.10	−0.44	0.65 ± 0.14	−0.02
λ4129	0.49 ± 0.07	−1.57	0.56 ± 0.07	−0.45	0.56 ± 0.09	+0.01
λ4205	0.48 ± 0.04	−1.54	0.60 ± 0.06	−0.43	0.55 ± 0.05	+0.04

splitting of ^{151}Eu is larger than that of ^{153}Eu, the asymmetry of the line profile increases with increasing fr(^{151}Eu).

Our measurements were carried out using the same procedure as was utilized for *r*-process–enhanced stars in Aoki et al. (2003). We searched for the isotope fractions that minimize the value of χ_r^2 for a given Eu abundance. We estimated the uncertainty of the derived Eu isotope fractions and total abundances by considering the range over which the χ_r^2 is twice as large as the best-fit case.[10] The error in the isotope fraction due to the uncertainty in the total Eu abundance was estimated from the range of the isotope fraction allowed within the adopted abundance uncertainty.

We estimated the errors arising from the following factors using the same procedures as in Aoki et al. (2003): (1) the macroturbulent velocity (given in Table 1), (2) the continuum-level uncertainty estimates, which are assumed to be 0.5% for HD 6268 and 1% for the other two stars, and (3) the wavelength calibration of the spectrum and the Eu line position. The wavelength shift was estimated from the longer wavelength (redder) part of the spectral line, which is insensitive to the Eu isotope ratio; the error is typically a few milliangstroms.

We analyzed three Eu II lines at 3819, 4129, and 4205 Å. Table 2 gives the derived ^{151}Eu fraction and total error ($\sigma_{\rm total}$), estimated from the quadrature sum of the individual errors mentioned above. The Eu (^{151}Eu + ^{153}Eu) abundance derived from each line is also given in the table. The λ4205 line is most sensitive to the Eu isotope fractions. Therefore, the fractions deduced from this line have the smallest uncertainty, even though the strong CH line at 4204.75 Å affects the bluest part of the Eu II line. The λ3819 line is strongest among the three lines. However, the uncertainty in the derived isotope ratio due to the error in the Eu abundance estimation is significant (Aoki et al. 2003). The Eu II λ4129 line, as for Eu II λ4205, has suitable strength for this analysis. However, our synthetic spectra fail to well reproduce the blue portion (~4129.6 Å) of the absorption line in the two carbon-rich stars. There seems to exist some unidentified absorption lines. Excluding the blue wing from the fitting, we derived the isotope fractions, given in Table 2, for the range of 4129.65–4129.82 Å. Although the number of data points within this range is sufficient, the results are rather sensitive to the choice of wavelength range used for the analysis.

For these reasons, we prefer to adopt the isotope fractions derived from the Eu II λ4205 line as the best determination. We note, for comparison purposes, that the weighted means of the results from all three lines for HD 6268, LP 625−44, and CS 31062−050 are 0.47, 0.61, and 0.57, respectively, which agree well with the results from the 4205 Å line alone.

The fr(^{151}Eu) of HD 6268 (0.48 ± 0.04) perfectly agrees with that of solar system material (0.478; Anders & Grevesse 1989), as found in other *r*-process element–enhanced stars (Sneden et al. 2002; Aoki et al. 2003). In contrast, the fr(^{151}Eu) of the two stars enriched in *s*-process elements are higher than the solar system value.

[10] This corresponds to approximately a 3 σ confidence level for 25 degrees of freedom, which is the case of our analysis for Eu lines. We do not, however, insist on the exact value of the confidence level, because the statistical properties are not proven for spectra rebinned to a constant wavelength step (Bonifacio & Caffau 2003).

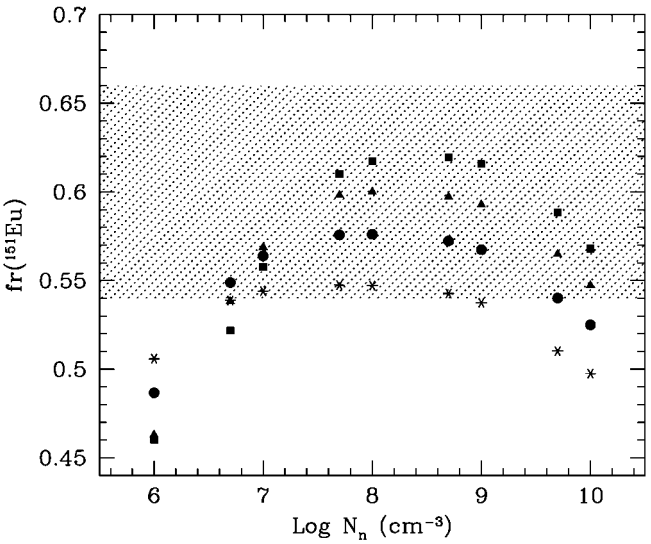

FIG. 2.—The fr(^{151}Eu) values calculated for four temperatures (*squares*: kT = 30 keV; *triangles*: 20 keV; *circles*: 15 keV; *asterisks*: 10 keV) as a function of neutron density (N_n). The fr(^{151}Eu) of LP 625−44 and its uncertainty is shown by the hatched area.

4. DISCUSSION

The yields of the *s*-process nuclides that explain the abundances of pure *s*-process isotopes in solar system material have been calculated by Arlandini et al. (1999). The fr(^{151}Eu) values deduced from their best-fit stellar and classical models are 0.541 and 0.585, respectively. The first conclusion of the present investigation is that the agreement between these values and those derived from our observations is quite good.

In order to further investigate what can be learned about the *s*-process from the measured Eu isotopes, we have made an analysis using the thermally pulsed *s*-process models described in Howard et al. (1986). We utilized updated neutron capture rates (e.g., Bao et al. 2000). In particular, in order to follow the nuclear flow in the Sm-Eu-Gd region, we included the rates for ^{151}Eu–^{155}Eu and ^{151}Sm obtained by Best et al. (2001) and Toukan et al. (1995). The electron capture rate of ^{153}Gd was adopted from Takahashi & Yokoi (1987). We found that the fr(^{151}Eu) value has almost no dependence on the mean neutron exposure (τ_0) for a fixed temperature in the range of $0.2 \leq \tau_0 \leq 0.8$, which well covers the τ_0 (~0.5 mbarn^{-1}) estimated by Aoki et al. (2001) for LP 625−44. Our results are calculated with $\tau_0 = 0.3$ mbarn^{-1}, which gives a good fit to solar abundances.

Figure 2 shows the fr(^{151}Eu) values calculated by our model. They are plotted as a function of neutron density (N_n) for four

temperatures (kT = 10, 15, 20, and 30 keV). Also shown for comparison by the hatched area is the fr(^{151}Eu) range deduced for the *s*-process element–enhanced star LP 625−44. As can be seen in this figure, the fr(^{151}Eu) value is rather sensitive to the ambient temperature and neutron density during the *s*-process. The fr(^{151}Eu) value is maximized in the range of neutron density from $N_n = 5 \times 10^7$ to 10^9 cm^{-3}.

The branching factor at ^{151}Sm is given by $f = \lambda_n/(\lambda_\beta + \lambda_n)$, where $\lambda_n = N_n v_T \langle\sigma\rangle$ and $\lambda_\beta = \ln 2/t_{1/2}$ are the neutron capture rate and the β-decay rate, respectively. In these formulations, v_T, $\langle\sigma\rangle$, and $t_{1/2}$ are the mean thermal velocity, the Maxwellian-averaged cross section, and the half-life, respectively. For $N_n > 10^7$ cm^{-3}, the branching factor is higher than 0.9. This indicates that the nuclear flow bypasses ^{151}Eu. In this case, the ^{151}Eu abundance is produced by the decay of ^{151}Sm after the neutron capture flow ceases. As the neutron density increases to $N_n > 10^9$ cm^{-3}, another branching at ^{153}Sm becomes important. Since we adopt a much smaller cross section for ^{153}Sm than those for ^{151}Sm and ^{153}Eu, the ^{153}Sm abundance relative to ^{151}Sm and ^{153}Eu *during* the neutron capture reactions increases with increasing neutron density. This results in a decrease of the *final* value of fr(^{151}Eu) with increasing neutron density for $N_n > 10^9$ cm^{-3}, as found in Figure 2. A measurement of the cross section for ^{153}Sm is thus highly desirable to constrain the high neutron density branching.

In contrast to the high neutron density conditions, ^{151}Sm β-decay *during* the *s*-process is increasingly important with decreasing neutron density ($N_n \lesssim 10^7$ cm^{-3}). For the typical temperature ranges thought to apply in the *s*-process (10–30 keV), the neutron capture rate on ^{151}Eu is faster than that for ^{153}Eu. Therefore, the nuclear flow passes through ^{151}Eu rather easily and creates ^{153}Gd via ^{151}Eu(n, γ) ^{152}Eu(β, ν)^{152}Gd(n, γ)^{153}Gd. In low neutron density conditions, the electron capture on ^{153}Gd is comparable with, or faster than, the neutron capture. This contributes to the production of ^{153}Eu and explains the decrease of fr(^{151}Eu) with decreasing neutron density in the low ($N_n \lesssim 10^7$ cm^{-3}) range. This trend appears more clearly for the higher temperature case, because the effect of a higher neutron capture rate on ^{151}Eu relative to that on ^{153}Eu is large, while the branching factor decreases with increasing temperature.

The comparison of the calculations with the observational results indicates that *s*-processes with high neutron density ($\log N_n \gtrsim 9$) and low temperature ($kT \lesssim 20$ keV), or those with quite low neutron density ($N_n < 10^7$ cm s^{-1}), are not allowed. This is a new constraint on *s*-process nucleosynthesis provided by the Eu isotope analysis.

Recent models of AGB stars show that the abundance patterns of nuclei in branchings are affected by the *s*-process both during the thermal pulses and between pulses (e.g., Arlandini et al. 1999). The reaction that provides neutrons in the former phase is ^{22}Ne(α, n)^{25}Mg, which produces a neutron density as high as 10^8–10^{10} cm^{-3}. In the interpulse phase, ^{13}C(α, n)^{16}O is assumed to be the neutron source reaction, which leads to a lower neutron density ($N_n \sim 10^7$ cm^{-3}). The observational errors of the derived Eu isotope fractions are still too large to constrain the contribution of each process to the final abundance patterns produced by nucleosynthesis in AGB stars. However, our analysis shows that Eu isotopes can be a new probe to determine the temperature and neutron density in *s*-process nucleosynthesis.

We note that the fr(^{151}Eu) values derived by using the previous nuclear data of Sm and Eu isotopes, in particular the ^{151}Sm neutron capture rate, are significantly lower than the results shown above. The previous neutron capture rate recommended by Bao et al. (2000), e.g., 2377 mbarn at 30 keV, is significantly higher than the rate used in the present work (1585 mbarn at 30 keV; Best et al. 2001). The high neutron capture rate causes the nuclear flow to bypass ^{151}Eu and results in lower fr(^{151}Eu) values by 0.05–0.08. The low neutron capture rate is clearly preferable to explain our observational results. New experiments to determine the neutron capture cross section of ^{151}Sm are highly desirable to fix ratios of ^{151}Eu/^{153}Eu and also ^{152}Gd/^{154}Gd.

It should also be noted that the Eu isotope fractions are quite similar between LP 625−44 and CS 31062−050, even though their Pb/Ba abundance ratios are significantly different (Aoki et al. 2002a, 2002b). This observational fact indicates that nuclear flow is very fast, and fr(^{151}Eu) easily obtains asymptotic values in the Sm-Eu-Gd region, once the flow passes through the $N = 82$ neutron magic nuclei. This situation is quite likely to occur in these very metal poor stars because of the expected high neutron-to-seed ratio. However, the Pb abundance is very sensitive to the neutron exposure (e.g., Gallino et al. 2003), and large variations of the Pb/Ba ratio are expected. Similar studies of additional *s*-process–enhanced stars would be useful to derive more clear conclusions on production of heavy nuclei by the *s*-process.

REFERENCES

Anders, E., & Grevesse, N. 1989, Geochim. Cosmochim. Acta, 53, 197
Aoki, W., Honda, S., Beers, T. C., & Sneden, C. 2003, ApJ, 586, 506
Aoki, W., Norris, J. E., Ryan, S. G., Beers, T. C., & Ando, H. 2000, ApJ, 536, L97
Aoki, W., Ryan, S. G., Norris, J. E., Beers, T. C., Ando, H., & Tsangarides, S. 2002a, ApJ, 580, 1149
Aoki, W., et al. 2001, ApJ, 561, 346
———. 2002b, PASJ, 54, 427
Arlandini, C., Käppeler, F., Wisshak, K., Gallino, R., Lugaro, M., Busso, M., & Straniero, O. 1999, ApJ, 525, 886
Bao, Z. Y., Beer, H., Käppeler, F., Voss, F., Wisshak, K., & Rauscher, T. 2000, At. Data Nucl. Data Tables, 76, 70
Beer, H., & Macklin, R. L. 1988, ApJ, 331, 1047
Best, J., et al. 2001, Phys. Rev. C, 64, 015801
Bonifacio, P., & Caffau, E. 2003, A&A, 399, 1183
Burris, D. L., Pilachowski, C. A., Armandroff, T. E., Sneden, C., Cowan, J. J., & Roe, H. 2000, ApJ, 544, 302
Cayrel, R., et al. 2001, Nature, 409, 691
Gallino, R., et al. 2003, Nucl. Phys. A, 718, 181c
Goriely, S., & Mowlavi, N. 2000, A&A, 362, 599
Howard, W. M., Mathews, G. J., Takahashi, K., & Ward, R. A. 1986, ApJ, 309, 633
Johnson, J. A., & Bolte, M. 2002, ApJ, 579, L87
Käppeler, F., Beer, H., & Wisshak, K. 1989, Rep. Prog. Phys., 52, 945
Kurucz, R. L. 1993, CD-ROM 13, ATLAS9 Stellar Atmospheres Programs and 2 km/s Grid (Cambridge: SAO)
Kurucz, R. L., & Bell, B. 1995, CD-ROM 23, Atomic Line List (Cambridge: SAO)
Lawler, J. E., Wickliffe, M. E., Den Hartog, E. A., & Sneden, C. 2001, ApJ, 563, 1075
Noguchi, K., et al. 2002, PASJ, 54, 855
Sneden, C., Cowan, J. J., Lawler, J. E., Burles, S., Beers, T. C., & Fuller, G. M. 2002, ApJ, 566, L25
Straniero, O., Gallino, R., Busso, M., Chieffi, A., Raiteri, C. M., Limongi, M., & Salaris, M. 1995, ApJ, 440, L85
Takahashi, K., & Yokoi, K. 1987, At. Data Nucl. Data Tables, 36, 375
Toukan, K. A., Debus, K., Käppeler, F., & Reffo, G. 1995, Phys. Rev. C, 51, 1540
Wisshak, K., Voss, F., Käppeler, F., Guber, K., Kazakov, L., Kornilov, N., Uhl, M., & Reffo, G. 1995, Phys. Rev. C, 52, 2762